Experimental Mechanics (2021) 61:1069–1080
https://doi.org/10.1007/s11340-021-00742-5

RESEARCH PAPER

Microindentation of Cartilage Before and After Articular Loading in a Bioreactor: Assessment of Length-Scale Dependency Using Two Analysis Methods

C. Yuh[1] · C. S. O'Bryan[2,3] · T. E. Angelini[2] · M. A. Wimmer[1]

Received: 24 November 2020 / Accepted: 4 June 2021 / Published online: 23 June 2021

Abstract

Background Microindentation is a technique with high sensitivity and spatial resolution, allowing for measurements at small-scale indentation depths. Various methods of indentation analysis to determine output properties exist.

Objective Here, the Oliver-Pharr Method and Hertzian Method were compared for stiffness analyses of articular cartilage at varying length-scales before and after bioreactor loading.

Methods Using three different conospherical tips with varying radii (20, 100, 793.75 μm), a bioreactor-indenter workflow was performed on cartilage explants to assess changes in stiffness due to articular loading. For all data, both the Oliver-Pharr Method and Hertzian Method were applied for indentation analysis.

Results The reduced moduli calculated by the Hertzian Method were found to be similar to those of the Oliver-Pharr Method when the 20 μm tip size was used. The reduced moduli calculated using the Hertzian Method were found to be consistent across the varying length-scales, whereas for the Oliver-Pharr Method, adhesion/suction led to the largest tip exhibiting an increased average reduced modulus compared to the two smaller tips. Loading induced stiffening of articular cartilage was observed consistently, regardless of tip size or indentation analysis applied.

Conclusions Overall, geometric linearity is preserved across all tip sizes for the Hertzian Method and may be assumed for the two smaller tip sizes using the Oliver-Pharr Method. These findings further validate the previously described stiffening response of the superficial zone of cartilage after articular loading and demonstrate that the finding is length-scale independent.

Keywords Articular Cartilage · Soft Matter · Microindentation · Stiffness · Biotribology

Introduction

Mechanical properties of articular cartilage have been investigated using indentation testing for decades [1], with the technique gaining significant momentum since the advent of micro- and nanoindentation systems in the early 2000s [2–4]. Instrumented small-scale indentation is a testing technique with high sensitivity and spatial resolution, allowing for measurements at nano- and micro-scale force levels in the assessment of hierarchal structures of materials. As the name suggests, microindentation can be simply described as a mechanical test that is performed using a micron-sized indenter and/or small indent depths, allowing for the determination of the properties of the microstructure of materials. This method is specifically useful for determining the penetration force versus the indentation depth of materials and has been useful in multiple fields of materials science [5].

In the case of biological soft tissues and biomimetic materials, such as hydrogels, extensive research efforts have been made towards improving indentation protocols for the purpose of developing indentation material models to find potential relationships between mechanical, structural, and

✉ C. Yuh
catherine_yuh@rush.edu

C. S. O'Bryan
csobryan@seas.upenn.edu

T. E. Angelini
t.e.angelini@ufl.edu

M. A. Wimmer
Markus_A_Wimmer@rush.edu

[1] Rush University Medical Center, Chicago, IL, USA

[2] University of Florida, Gainesville, FL, USA

[3] University of Pennsylvania, Philadelphia, PA, USA

biochemical properties of the tissue [6–9]. Microindentation has also been used to determine changes in the tissue undergoing experimental or pathological induction [5]. Such studies include investigating the mechanical differences between osteoarthritic vs. healthy tissue, and/or assessing the effect of advanced glycation end products crosslinking on cartilage stiffness [10, 11]. Our own studies addressed transient stiffening of the superficial zone cartilage after articulation and loading [12]. These demonstrate that microindentation is a sensitive technique capable of detecting such biochemical changes at the micron-level.

Although microindentation has been used extensively to assess the mechanical properties of articular cartilage (over 120 papers in PubMed), multiple challenges still remain. One particular challenge is determining the appropriate analysis method. The Oliver-Pharr Method [13] is considered the "gold standard" analytical method for materials that exhibit classical stress–strain curves, such as metals. This method is applied to the unloading portion of the load–displacement curve, which isolates the elastic response from material plastic yielding. Therefore, in a biphasic material, such as articular cartilage, by focusing on the unloading portion of the curve, the output stiffness is that of the solid phase and does not account for the fluid contribution towards the tissue's behavior. In articular cartilage, the highly biphasic nature of the tissue [9, 14] and the intrinsic viscoelasticity of the collagen network [6] result in time-dependent and non-linear material behaviors at given indentation input parameters (e.g., high indentation strains), all of which are factors that can invalidate the linearity assumptions that are used in the Oliver-Pharr Method. The non-linearity of the tissue results in a length-scale dependency of the tissue, as indentation output calculations are dependent on the contact area between the indenter and the sample surface.

Another commonly used elastic contact model, the Hertzian Method, fits along the loading portion of the load–displacement curve. By focusing on the loading portion, the Hertzian Method does not isolate the elastic response of the sample as the Oliver-Pharr Method does. Thus, the output stiffnesses measured using the Hertzian Method is a combined stiffness that includes both the stiffness contributions of the fluid phase and solid phase. Additionally, in soft and/or hydrated materials, accurate determination of the point of contact on hydrated soft materials can be challenging. For example, in addition to noise, the surrounding fluid can interfere in defining the point of contact on low elastic moduli materials, in that forces from the fluid, instead of the sample, are incorrectly detected. This leads to inaccuracies in calculations of output stiffness measurements. A recent publication by Garcia et al. identified a relationship between the first derivative of the force relative to the displacement to determine the Hertzian elastic modulus without requiring the local displacement of the point of contact [15], therefore improving the accuracy of indentation output measurements.

One particular challenge of both of these contact models includes artifacts introduced by adhesive contact or suction during the indentation protocol, especially when indenting soft materials. Adhesion can be a result of structural-chemical adhesive binding effects between the sample and the tip, whereas suction is due to the formation of a vacuum in biphasic materials as fluid movement occurs during the indent [16, 17]. In either condition, the tip to sample contact during indentation can be affected by "jumps" into and out of contact. In the Oliver-Pharr Method, since analysis is performed on the unloading portion of the curve, a "jump" depicted by a sharp drop of force induced by adhesion or suction can lead to an overestimation of stiffness. Alternatively, when using the Hertzian method, adhesion can cause a "jump" into contact, making it difficult to determine the true point of contact, also leading to erroneous calculations of mechanical properties. Indentation artifacts such as adhesion and suction effects may be length-scale dependent [16, 18], and it is important to avoid using input parameters that would lead to such an erroneous response. Despite these caveats, both models have been used in the mechanical characterization of soft tissues and materials and the identification of changes in properties due to various complex experimental conditions [10, 11, 15, 19].

In this body of work, it was of interest to use microindentation to assess whether the mechanical surface properties of cartilage are affected by stresses induced by joint loading and articulation, with the overarching goal to further the understanding of structure–function relationships at various length-scales. It has been consistently reported that the effects of loading and sliding can have major implications on tissue function and health [20–23]. In our previous work [12], we observed that articular cartilage exhibits a stiffening response after combined articular loading. Most notably, we found that this response is specific to the superficial layer of the tissue. The loss of this response when the surface is removed may indicate that this articulation-induced stiffening response may be important in keeping cartilage tribologically sustainable during articular loading.

Therefore, the purpose of this presented work was to perform a follow up study to provide additional verification of the articular loading-induced stiffening response. More specifically, the goals of this study were to determine how both cartilage stiffness and articular loading-induced stiffening would respond when varying the indentation length-scale and when using different indentation analysis methods. To achieve this, microindentation was performed before and after tissue testing in a bioreactor that mimics joint loading and articulation [12, 24]. Length-scale dependencies were investigated by using conospherical tips of various radii.

We also sought to compare the Oliver-Pharr Method, which assesses the stiffness parameters in the unloading phase, to the Hertzian Method, which assesses the stiffness parameters in the loading portion of the curve. To mitigate challenges in detecting an accurate contact depth (due to noise, "jump into contact" from adhesion, etc.), we used the modified Hertzian Model described in Garcia et al. [15].

Theory

For analyzing static indentation curves, two commonly used elastic contact analysis methods include the Oliver-Pharr Method and the Hertzian Method to determine the reduced modulus (E*). These methods assume an isotropic, time-independent, and elastic material model during indentation testing. As E* is the "effective" or "reduced" modulus, this parameter also accounts for both the material of interest's and the indenter's elastic moduli (E) and Poisson's ratios (ν), and is also defined as:

$$\frac{1}{E^*} = \left(\frac{1-\nu^2}{E}\right)_{cartilage} + \left(\frac{1-\nu^2}{E}\right)_{indenter} \tag{1}$$

Because cartilage is a relatively soft material, the indenter material, such as the commonly used diamond or sapphire, is usually much stiffer. Thus, the resulting E* can be considered to be comparable to the value of $\frac{E_{cartilage}}{1-\nu^2}$.

Hertzian Method

The Hertzian Method is a classically used elastic contact model used in indentation analysis, first determined in 1882 by Heinrich Hertz [25]. The Hertzian relationship between force P and displacement h when using a spherical probe on an elastic half-space was defined as [26]:

$$P = \left(\frac{4}{3}\right)\left(E^* R^{\frac{1}{2}}\left(h-h_0\right)^{\frac{3}{2}}\right) \tag{2}$$

where h_0 is the displacement at which contact is made between the indenter and the sample, and R is the radius of the spherical tip. This method is based on Hooke's law, and therefore follows linear elasticity assumptions. More than half a decade later, in 1951, David Tabor empirically determined the average indentation stress σ^* and indentation strain ε^* in metals, with a as the contact radius [27]:

$$\sigma^* = \frac{P}{\pi a^2} \tag{3}$$

$$\varepsilon^* = \frac{0.2a}{R} \tag{4}$$

Because the exact initial point of contact between the indentation tip and the substrate can be difficult to determine for cartilage and other soft materials, a modified Hertzian Contact model was used for the analysis. Here, the traditional Hertzian force–displacement model is recast in terms of the first-derivative of the contact force with respect to the indenter position. This modification presented in Garcia et al. removes the need to input the initial point of contact h_0 to determine E*, and is defined as:

$$P' = \frac{3}{2}\left(\left(\frac{4}{3}\right)\left(E^* R^{\frac{1}{2}}\right)\right)^{\frac{2}{3}} P^{\frac{1}{3}} \tag{5}$$

Oliver-Pharr Method

In 1992, Oliver and Pharr published an experimentally determined method to define the E* using the force–displacement relationship determined by Sneddon in the mid-1900s [13]. Sneddon's model defines the relationship between the force P and displacement h as a power-law fit of initial portion of the unloading phase, where α and m are the power-law fit coefficients, and h_f is the final depth [28]:

$$P = \alpha\left(h-h_f\right)^m \tag{6}$$

By fitting a load–displacement curve to this power-law in Eq. 6, the initial stiffness S can be calculated at the beginning of the fitted region on the unloading phase by taking the derivative of the force respective to the displacement:

$$S = \frac{dP}{dh} \tag{7}$$

In spherical indentation, using either a theoretical or experimentally obtained tip area function $A(h_c)$, where h_c is the depth of the indenter in contact with the sample and R is the radius of a conospherical tip, the E* can be calculated from the following equations:

$$A\left(h_c\right) = -\pi\left(h_c\right)^2 + 2\pi R\left(h_c\right) \tag{8}$$

$$E^* = \frac{S\sqrt{\pi}}{2\sqrt{A(h_c)}} \tag{9}$$

Length-Scale Dependency and Linearity Assumptions

It is important to note that the elastic models used in the indentation analysis methods presented here assume linearity [29]. More specifically, in a non-linear material, such as cartilage or other soft hydrated materials, the linear

range of the load–displacement curve would be defined as a range of indentation strains where the resultant contact area A_c has a linear relationship with the resultant stiffness S. Therefore, in this linear range, the output E* measurements should be the same regardless of indentation strain applied. In the context of this particular length-scale experiment, geometric linearity was assessed through using varying tip sizes. As the tip size used increases, the contact area between the sample and the tip also increases, therefore changing the underlying indentation strain in the contact. In order to use either the Oliver-Pharr Method or the Hertzian Method, it is imperative to meet this linearity assumption to obtain accurate measurements of E*. Therefore, an aim of this particular study was to assess cartilage E* at varying length-scales before and after articular loading to assess whether the responses observed were within the linear range necessary to use the presented contact models for analysis.

Experimental Procedures

Tissue Procurement and Materials

Eighteen articular cartilage 14 × 20 × 3 mm oval explants from six live 6–8-month-old bovine stifle joints were removed from the subchondral bone of the trochlear groove. All explants were removed from the trochlear groove of each stifle joint using a custom oval punch and placed into fresh 1 × PBS at 4 °C until the day of testing (no more than 24–48 h after procurement). From each animal, three explants were removed and distributed into three experimental groups that represent the conospherical indenter sizes that were used for this study: 20 μm, 100 μm, and 793.75 μm (1/16″) radii tips (n = 6). The tip material of the largest tip was alumina, whereas the other two tip materials used were diamond.

Microindentation Protocol

In this study, microindentation stress-relaxation curves were obtained using the Hysitron TI 950 Nanoindenter (Bruker Inc, Minneapolis, MN) (Fig. 1). Prior to indentation, the explants were fixed using cyanoacrylate (Loctite® Gel Control Super Glue) to a custom PEEK sample holder that allows for sufficient clearance under the indenter transducer and for the addition of fluid to fully submerge the cartilage explant. The sample was then placed under a microscope optic in the indenter system to determine the point of indentation, where the local height of the indentation point was first determined without fluid in the sample holder. Once surface determination was complete, fluid was added back to fully submerge the explant. Indents were performed as an automation of 3 × 1 indents positioned 100 μm apart. The initial point of contact was determined by setting a 7.5 μN setpoint. The respective tip size for each sample was used based on the group that the sample was in (20 μm, 100 μm, or 793.75 μm).

For each indent, a static displacement-controlled indentation protocol was applied. In energy-dissipating materials, such as cartilage, applying a held strain leads to a decrease in load over time, characteristic of stress relaxation. Therefore, for this particular protocol, when contact was determined, a 0.75 μm tip retraction is initially applied, followed by a "loading phase" at 0.8 μm s^{-1} to a peak displacement of 8 μm, then a 60 s "hold phase" to allow for stress relaxation, followed by an "unloading phase" at -0.8 μm s^{-1} back towards 0 μm displacement.

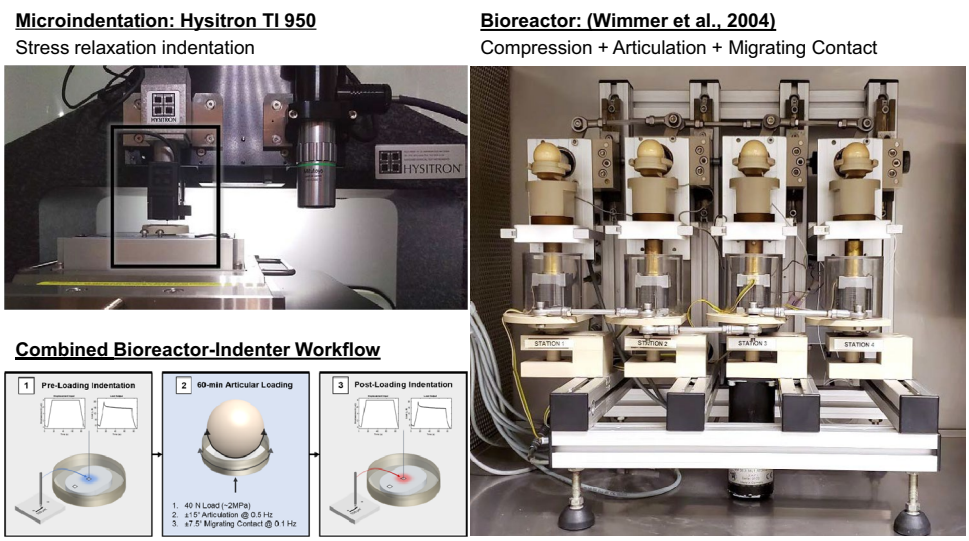

Fig. 1 A Hysitron TI 950 Nanoindenter (top-left) was used to perform displacement-controlled indentation. The input displacement and output load are shown (bottom). A custom bioreactor system (right) was used to apply articular load to cartilage explants. Together, these devices were used to perform a combined bioreactor-indenter workflow (bottom-left)

Bioreactor System

A dual-axial joint simulator capable of applying complex motion patterns onto cartilage explants was used to simulate joint articular loading in vivo (Fig. 1) [24, 30]. This system utilizes two rotational stepper motors and a linear stepper motor to apply various motions. One rotational motor applies articulation using an alumina 32-mm Ø hip ball intended to simulate sliding induced by motions such as flexion/extension of the knee or hip. The second rotational motor applies a curvilinear migrating contact path onto the cartilage explant, to simulate movements such as internal/external rotation and anterior/posterior translation. Together, these rotational motors are capable of replicating the varying combinations of sliding and rolling motions that exist in the knee joint. Finally, the linear actuator can provide either static or dynamic compression onto the cartilage explants, with 40 N approximately equivalent to 2 MPa of contact pressure, as observed in the knee joint [31].

Altogether, static 40 N confined compression and 0.5 Hz of ± 15° articulation from a 32-mm Ø alumina hip ball is applied onto the cartilage explants. The alumina ball is migrated 5.2 mm across the cartilage surface at a frequency of 0.1 Hz. In this study, articular loading was performed submerged in fresh 1×PBS for 60 min.

Bioreactor-Indenter Workflow

For each explant, a bioreactor-indenter workflow [12] was performed (Fig. 1). On the day of testing, cartilage explants were fixed in position to the indentation sample holder using cyanoacrylate glue and placed in the indentation device for a baseline microindentation measurement in the center/contact and left/periphery regions. Following the initial stiffness assessment, the explant is gently removed from the indentation sample holder and placed into the bioreactor system for articular loading application against a 32-mm Ø alumina hip ball for 60 min. Immediately following bioreactor testing, the sample is transferred back to the indentation device, and the microindentation protocol is repeated in the center/contact and left/periphery regions.

Data Analysis

For indentation analysis, both the Oliver-Pharr Method and the Hertzian Method were performed for assessment of cartilage E*. Using the Oliver-Pharr Method, for each tip size, Eq. 8 was used to calculate each respective idealized area function $A(h_c)$. The Oliver-Pharr Reduced Modulus (E^*_{OP}) was calculated on the Oliver-Pharr power law fit of the 80–95% portion (i.e., beginning, see Fig. 2) of the unloading curve using the accompanied Hysitron Triboscan software. For the Hertzian Method, the modified relationship in Eq. 5

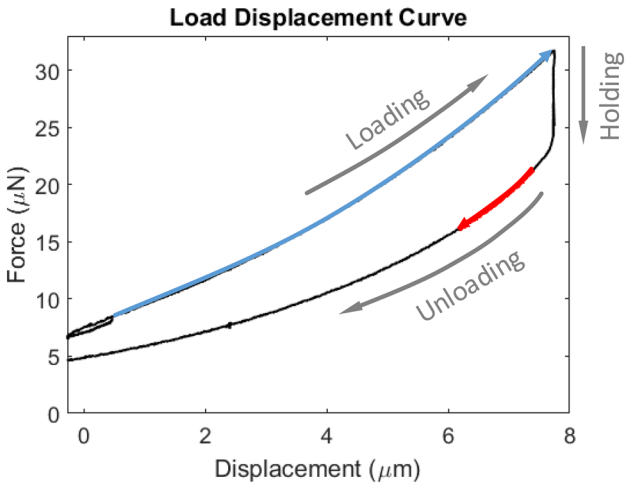

Fig. 2 Output load–displacement curve obtained during indentation. The portion of the unloading phase from which the Oliver-Pharr stiffness is measured is highlighted in red. The portion of the loading phase where the Hertzian Model is fit is shown in blue. Note that the force at the end of the load–displacement curve does not return to the setpoint value of 7.5 μN (due to relaxation of the tissue).

was applied to the linear portion of the loading phase to calculate the Hertzian Reduced Modulus (E^*_{Hz}).

All statistical analyses were performed using Design Expert 13 (Stat-Ease Inc., Minneapolis, MN) and SPSS v22 (IBM, Armonk, NY). Normality and homoscedasticity were confirmed using a Shapiro Wilks Test and Levene's Test, respectively. The data were then analyzed using a two factor-interaction 4-way ANOVA model ($n = 6$, Power > 80% for all model factors). More specifically, the four input factors of this ANOVA model were tip radius (20 vs. 100 vs. 793.75 μm), bioreactor testing (before vs. after), region on the explant (contact vs. periphery), and analysis method utilized (Oliver-Pharr Method vs. Hertzian Method), while our output variable for this ANOVA model was E*. Post-hoc tests were performed to assess statistically significant differences between tip radii using Bonferroni corrections. Because all other factors (except tip radius) only had two levels, the resulting main effects were sufficient to indicate if a significant difference exists for these factors without need of further post-hoc tests. For all analyses, the significance level was defined as $\alpha = 0.05$.

Results

4-way ANOVA Model Results

The statistical model generated using a 4-way ANOVA was found to be highly significant ($p < 0.0001$) overall. All main effect terms (Tip Radius, Bioreactor Testing, Analysis Method, and Region) were found to be significant. Only two interaction

Table 1 4-way ANOVA Model Terms and Significance

Term	p-value
Model	$p<0.0001$
Tip Radius	$p<0.0001$
Bioreactor Testing	$p=0.0019$
Analysis Method	$p<0.0001$
Region	$p=0.0140$
Tip Radius × Bioreactor Testing	$p=0.1749$
Tip Radius × Analysis Method	$p<0.0001$
Tip Radius × Region	$p=0.9438$
Bioreactor Testing × Analysis Method	$p=0.9142$
Bioreactor Testing × Region	$p<0.0001$
Analysis Method × Region	$p=0.8371$

terms, [Tip Radius × Analysis Method] and [Bioreactor Testing × Region] were observed to be significant. All model terms and their associated p-values can be found in Table 1.

Length-Scale Dependency of Cartilage Indentation Stiffness at Baseline

Bonferroni post-hoc comparisons were performed to assess differences between the tip radii used in this study. First, it was of interest to assess whether there exists a length-scale dependency on baseline indentation results (no applied articular load) for each analysis method. Based on post-hoc comparisons of baseline (pre-articulation) E^*_{OP} values from the resulting 4-way ANOVA model, no significant differences were observed between the E^*_{OP} obtained using the 20 and 100 μm tip radii within either the contact ($p>0.05$) or the periphery regions ($p>0.05$). On the other hand, it was found that the E^*_{OP} values of the largest tip size were on average significantly larger compared to both of the smaller tip sizes (100 vs. 793.75: $p=0.0024$ and 20 vs. 793.75: $p=0.0190$) (Fig. 3a). In contrast, using the Hertzian Method, fitting the data from the loading phase, it was found that the E^*_{Hz} of all three tip groups were more comparable to each other than what was observed using the Oliver-Pharr Method. Most notably, it was observed that the largest tip size exhibited no significant differences in E^*_{Hz} compared to either of the smaller tip sizes ($p>0.05$) (Fig. 3b).

Upon further inspection, it was found that the load–displacement curves of the 793.75 μm tip group exhibited a "jump out of contact" indicating an adhesion and/or suction artifact, depicted as a fast decrease in load leading to negative force at the beginning of the unloading phase (Fig. 4, top-right panel). The large E^*_{OP} found in this particular group was therefore attributed to an overestimation due to this response. Interestingly, the loading curves for all indents indicated no "jump into contact", which would be characteristic of an adhesion response. Therefore, we assume,E^*_{Hz} has not been affected by these artifacts. E^*_{OP} values were also generally observed to be significantly larger (approximately double) compared to the E^*_{Hz} values within the same groups and regions (except for that of the largest tip due to the overestimation of E^*_{OP}).

(a)

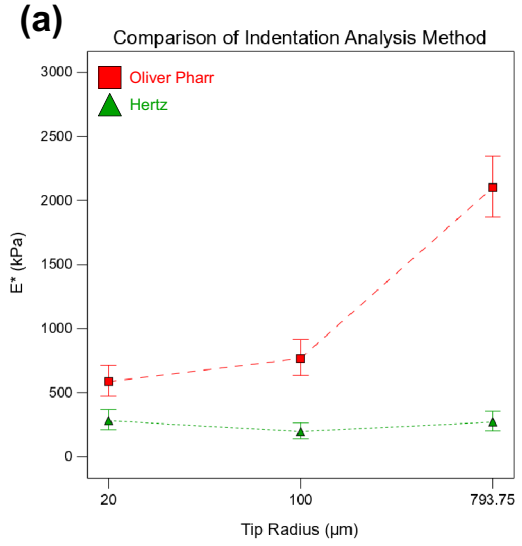

(b)

Contact Region

Tip Comparison	Oliver-Pharr Significance	Hertzian Significance
20 vs. 100	p>0.05	p>0.05
100 vs. 793.75	**p=0.0024**	p>0.05
20 vs. 793.75	**p=0.0190**	p>0.05

Periphery Region

Tip Comparison	Oliver-Pharr Significance	Hertzian Significance
20 vs. 100	p>0.05	p>0.05
100 vs. 793.75	**p=0.0021**	p>0.05
20 vs. 793.75	**p=0.0086**	p>0.05

Fig. 3 **a** Interaction plot showing baseline average E* ± Least Significant Difference 95% Confidence Interval values using the Oliver-Pharr Method (red squares) and Hertzian Method (green triangles). Averages were taken for all indents performed on each explant before articular loading was applied. **b** Post-hoc tests were performed to assess significant differences between tip radii for each analysis method within each region. Note that Fig. 3a visualizes the pooled data from both the contact and periphery regions

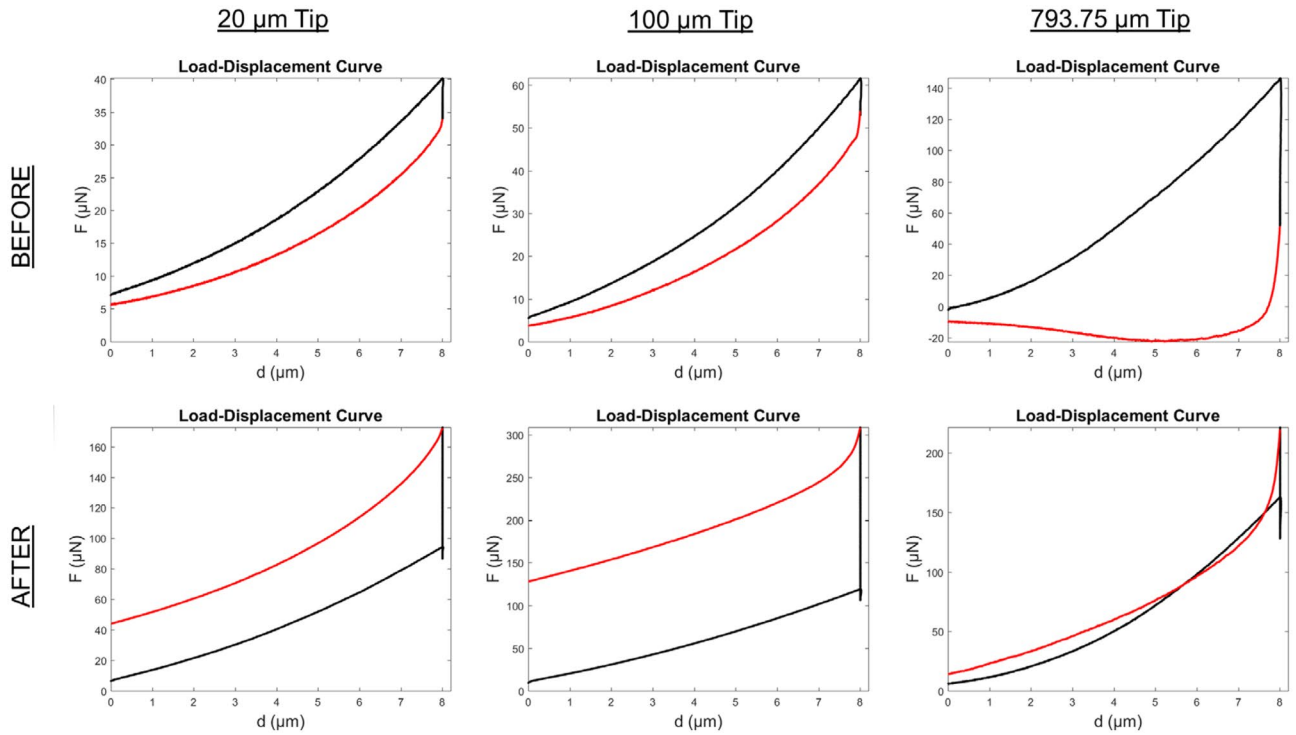

Fig. 4 Representative curves for each tip group, before and after bioreactor testing. The unloading phase for each plot is depicted in red. In the largest tip group, there is a clear "jump out of contact" artifact present in the unloading phase of the load–displacement curve prior to articular loading (top-right panel)

Finally, because a highly significant interaction effect of [Tip Radius × Analysis Method] was observed in the 4-way ANOVA results, comparisons between analysis method (Oliver-Pharr Method vs. Hertzian Method) on baseline E* values at the varying tip sizes were assessed. E^*_{OP} and E^*_{Hz} were found to be non-significantly different only for the 20 μm tip size ($p > 0.05$). For the 100 and 793.75 μm tip sizes, there was a statistically significant difference between the Oliver-Pharr Method and Hertzian Method E* calculations ($p < 0.001$).

Verification of Geometric Linearity

Based on the baseline E* data, geometric linearity was confirmed for the strains applied by the 20 and 100 μm tip groups for E^*_{OP}. It is important to note that while the 793.75 μm tip group exhibited significantly larger E^*_{OP} values, as aforementioned, it is likely that this disparity is unrelated to non-linear material effects as geometric linearity was observed when using the Hertzian Method for all three tip sizes, as all tip groups demonstrated non-significant differences to each other ($p > 0.05$) in E^*_{Hz} in all indented regions prior to articular loading (Fig. 3b). Rather, we attribute this overestimation of E^*_{OP} to the "jump out of contact" between the indentation tip and the cartilage sample. These findings indicate that the use of any of these tip sizes, except in the case of the largest tip size for the Oliver-Pharr Method, at the nominal indentation depth of 8 μm fulfilled the linearity assumption necessary for both analysis methods.

Effect of Articular Loading on Cartilage Stiffness

The 4-way ANOVA indicated both the main effect for [Bioreactor Testing] and the interaction effect [Bioreactor Testing × Region] to be highly significant on cartilage E* (Table 1). Regardless of indentation contact model used and tip size, overall, the contact region of the tissue exhibited increased E* values after articulation compared to their respective baseline measurements, indicating a stiffening response (Fig. 5). In contrast, no stiffening response was observed for the periphery region before and after bioreactor testing. The average stiffening factors calculated by taking the ratio of average post-articulation E* divided by average pre-articulation E* (Post:Pre) for the contact region using the Oliver-Pharr Method were 4.73, 2.16, and 1.75, for the 20, 100, and 793.75 μm tips, respectively. Using the Hertzian Method, the related stiffening factors were found to be 3.88, 3.17, and 3.25. These values are depicted visually in Fig. 6 for the 20 and 100 μm tip sizes. No significant differences in the stiffening ratios were found ($p > 0.05$).

Finally, based on Bonferroni post-hoc comparisons between tip radii in the context of cartilage stiffening, when using the Oliver-Pharr Method, the resulting E^*_{OP} indicated that healthy

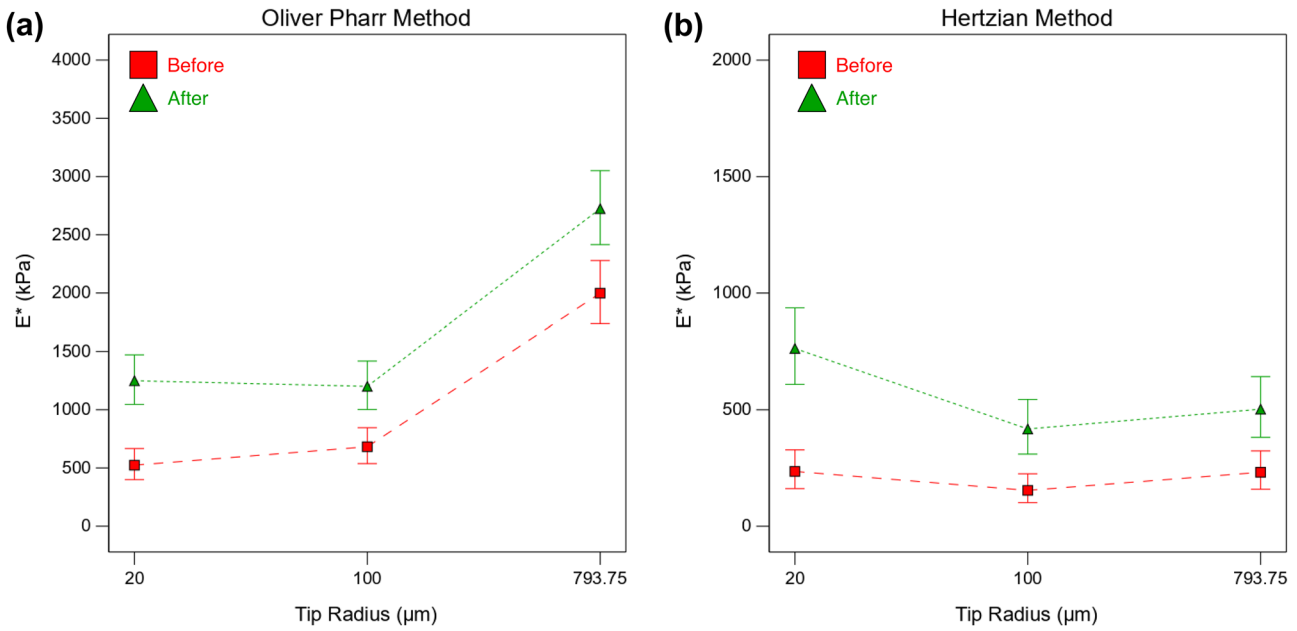

Fig. 5 Average ± Least Significant Difference 95% Confidence Intervals for **a** E^*_{OP} values calculated using the Oliver-Pharr Method and **b** E^*_{Hz} values calculated using the Hertzian Method

articular cartilage stiffnesses both prior to and after bioreactor testing is not significantly different between the 20 and 100 μm tip. Interestingly, clear adhesion and/or suction effects were only observed prior to bioreactor testing using the 793.75 μm probe and not after. On the other hand, using the Hertzian Method, no significant differences were found between E^*_{Hz} across all tip sizes, both before and after articular loading.

Finally, one notable finding observed after applied articular loading was an increase in force during the holding phase in the load–displacement curves (Fig. 4). It is important to note that the curves in the post-loading condition are, therefore, not representative of a traditional hysteresis which indicate energy dissipation, reflected by a loss of force during a displacement-controlled indent. Instead, the post-loading curves indicate an increase in force, which may be due to the swelling of the contact region, as fluid moves into the deformation induced by articular loading. Interestingly, this increase in force was only observed in the contact region, and not the periphery region.

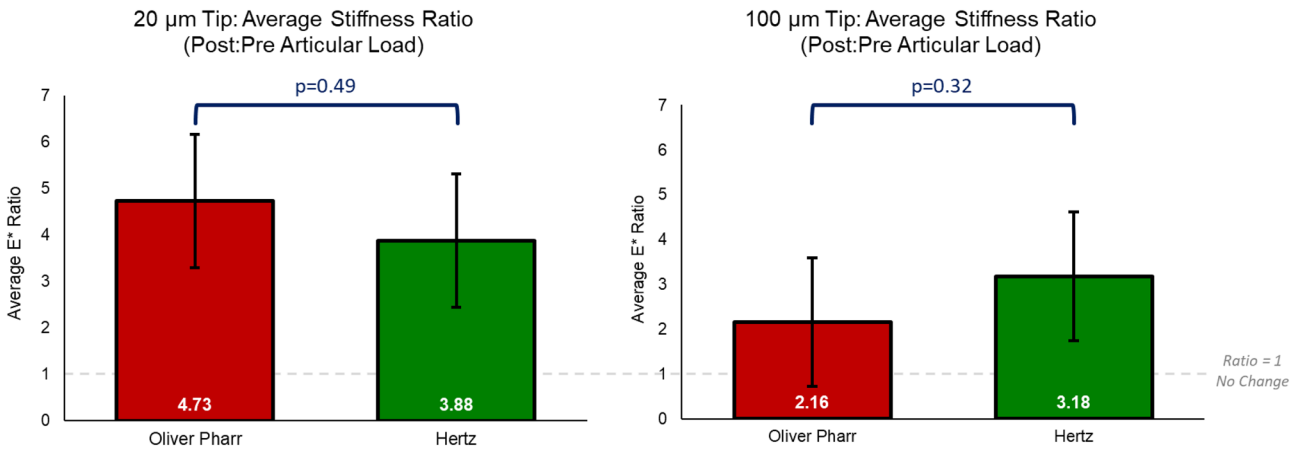

Fig. 6 Stiffness ratios for the 20 and 100 μm tip groups, comparing the Oliver-Pharr Method and the Hertzian Method. Note: The largest tip group (793.75 μm) is not included, due to the large adhesion/suction artifact found in the unloading phase

Discussion

In our previous publication, we found that the superficial zone of cartilage transiently increases in stiffness as a result of articular loading, with the stiffness returning towards baseline values within 3 h after articular loading [12]. This stiffening response was also found to be lost altogether when the superficial zone was removed. As this stiffening behavior is a unique feature of the superficial zone, this may point to a structure–function relationship that exists within this layer to maintain cartilage integrity at the surface during articular loading. The purpose of this presented study was to assess how articular loading-induced stiffening behaves at varying indentation length-scales. Articular cartilage stiffness and stiffening were also assessed using multiple indentation analysis methods to rule out measurement artifacts.

Specifically, cartilage surface stiffnesses were compared using two analysis methods, one following the model of Oliver-Pharr, and the other a modified Hertzian approach. Reduced elastic moduli E* were obtained before and after articular loading via a bioreactor system at varying length-scales. E* measurements were only comparable between both methods when the 20 μm radius tip was used. For larger tip sizes, the moduli obtained through the Oliver-Pharr Method were generally higher compared to those of the Hertzian Method. After articular loading was applied to explants, regardless of tip size, on average, all groups showed a stiffening response in the contact region of the tissue. Thus, this stiffening response does not appear to be length-scale dependent in the range of tip sizes tested and can be observed using two different contact models of indentation analysis. Altogether, the E* measurements from both techniques resulted in values that were within the ranges reported in the literature [9, 32–35].

The Oliver-Pharr Method obtains E* by using a power law fit to the unloading portion of the load–displacement curve. Thus, in theory, the effect of fluid is removed, and the resultant E* is that of the solid phase. Alternatively, the Hertzian Method fits to the loading phase, where fluid effects may still contribute to the resulting E* being measured. Further, the Oliver-Pharr Method utilizes an idealized contact area as a function of indent depth to determine E*, whereas the modified Hertzian Method [15] used herein does not rely on knowing the indent contact depth or area. This distinction may have contributed to the differences in the resulting E* measurements from each analysis method, particularly for the larger tip sizes.

The results also indicated that the indent depth of 8 μm led to baseline E* measurements that were not significantly different across the 20 and 100 μm tip sizes for both the Oliver-Pharr Method and the Hertzian Method. Similarly, the stiffness ratio before and after articular loading was found to be similar between both tip sizes and analysis techniques. The only tip group and analysis method that was found to result in measurements outside the linear range was the largest tip, 793.75 μm, using the Oliver-Pharr Method. Taken together, the protocol used in this study confirmed the linearity assumptions necessary for use of Oliver-Pharr for the 20 and 100 μm tip sizes. All three tip sizes fulfilled the assumptions for the Hertzian Method.

The load–displacement curves generated using the 793.75 μm tip exhibited an adhesion and/or suction artifact represented by a clear drop in force upon unloading in pre-bioreactor testing. Interestingly, however, this response was not apparent after bioreactor testing in the contact region. In addition, in the loading portion of the load–displacement curve, no "jump into contact" was observed in any of the indentation curves generated using the largest tip. Furthermore, the tip materials used in this study were diamond and alumina, both of which are highly inert materials that are significantly stiffer compared to cartilage. Based on these considerations, it is unlikely that the sharp drop to negative force depicted in the load–displacement curves was caused by molecular adhesion between the surfaces of the tip and the sample. Instead, we postulate that fluid exudation from the contact is responsible for this phenomenon. Fluid exudation can initiate the development of a vacuum during the retraction phase of the indenter, causing an adhesion-like suction response [16]. As the sharp drop in force in the unloading phase is not seen after articular loading is applied during bioreactor testing, it is likely that articular loading-induced swelling of the tissue outcompetes vacuum formation, thus, preventing a large suction effect from occurring. It is important to note, however, that this does not necessarily indicate that adhesion and/or suction was not present in the post-bioreactor condition. Rather, these responses on the load displacement curve were attenuated by a phenomenon such as articular loading-induced swelling. Therefore, the stiffness of the post-articular loading group for the largest tip size may not exhibit the same amount of overestimation compared to its respective baseline values.

In the context of the presented study, the modified Hertzian Method likely provides a more representative E* compared to the Oliver-Pharr Method. Although both methods resulted in E* values within the range reported by literature [9, 32–35], the modified Hertzian model presented by Garcia et al. [15] does not require knowing the displacement at the initial point of contact when calculating E*, thereby improving the accuracy by which these calculations are determined. Furthermore, the load–displacement curves presented in this study do not appear to have a "jump into contact" in the loading phase in any of the conditions and tip sizes tested. However, a characteristic adhesion/suction effect is present in the unloading phase when using the large alumina tip,

resulting in the overestimation of E* when using the Oliver Pharr Method. Therefore, using the modified Hertzian Method may provide a more accurate measurement of E* of the cartilage explants used in this study.

It is important to note, however, that a unique aspect of the presented study is the addition of simulated joint movement and loading to assess the effect of articular loading on the tissue's surface stiffness. Similar to what was observed in our previous study, articular loading was found to increase cartilage surface E* [12]. Most notably, the results of the presented study indicated non-significantly different stiffening ratios between the Oliver-Pharr Method and the Hertzian Method. Thus, these findings do not conclusively indicate that one analysis method is superior to the other for assessing cartilage stiffening induced by articular loading. Nonetheless, it is critical to consider that it may be advantageous to use one method versus the other, depending on the specific research questions being investigated.

For example, when studying the properties of the solid matrix, specifically, it may be advantageous to remove the effect of the fluid phase from the analysis, as is performed using Oliver-Pharr Method. It has been extensively demonstrated in the literature that alterations to the solid matrix can affect the stiffness response of cartilage [10, 11, 35–38], and it is ultimately the constituents and structure of the solid matrix that drive the fluid response of the tissue. When performed consistently without adhesion-like responses, the Oliver-Pharr Method can be useful to identify trends of changes in material properties of the solid phase as a result of experimental inputs [5]. For example, studies by McGann et al. and Moshtagh et al. investigated the effects of crosslinking by advanced glycation end products on the solid collagen network by using the Oliver-Pharr Method [10, 11]. However, it is important to note that, adhesion and/or suction effects can affect the indenter during retraction, leading to overestimations of E^*_{OP}, as observed here in this study. Such artifacts have been reported to be a primary challenge of indenting soft and hydrated materials [16, 17], such as cartilage, and careful considerations must be made in the testing set up to avoid measurement inaccuracies. This study suggests that smaller tip sizes are less prone to this artifact.

Moreover, there is irrefutable evidence that the fluid phase also plays a crucial role in the tissue's mechanical behavior. It has been previously shown that cartilage mechanical properties are dominated by highly non-linear biphasic properties, and that overall, the tissue does not follow models of linear poroelasticity (similar to that of agarose) or viscoelasticity [9, 39]. The dominance of the poroelastic response to mechanical loading highlight the crucial role of interstitial fluid pressurization as a result of tissue loading. This would promote the use of the Hertzian Method to study functional responses from the combined stiffness contributions of both the solid phase and fluid phase of the tissue. More recently, findings by Han et al. [6] suggested that the tissue also exhibits intrinsic viscoelasticity that is responsible for a baseline dissipation of the tissue, whereas fluid flow from poroelasticity increases the overall energy dissipation. This particular study used the principle that poroelasticity is length-dependent, whereas viscoelasticity is length-independent, and was also performed at multiple length-scales. As we did not observe a change in stiffening ratio across the length-scale assessed, this may indicate that the stiffening response may not be driven by poroelastic contributions of the tissue. Therefore, in future work, it would be interesting to assess the dissipative properties of the tissue in the context of the articular loading-induced stiffening response observed in this study.

One challenge of this study was performing indentation after applied articular loading during bioreactor testing and assessing the data appropriately. As observed in Fig. 4, during the holding phase of the indentation protocol, an increase in force is observed. This is a different response compared to the traditional hysteresis that is typically observed in indentation of soft dissipative materials. This increase in force may be potentially due to fluid movement into the contact area, which pushes the surface up during the indentation protocol. Therefore, it is important to consider that the E* measured after articular loading is not necessarily an absolute E*, as the tissue is not in its equilibrium state. With this consideration, one possible reason for the stiffening response from a contact mechanics perspective is the piling up or sinking in of the tip. In indentation analysis on a sample that has experienced pile up or sink in, the contact area and contact depths are altered, which in turn can cause an overestimation in E* [40]. However, in the presented study, pile-up effects would likely differ between the various tip sizes used. Instead, it was found that the ratio of articular loading-induced stiffening was non-significantly different between all three tip sizes, regardless of indentation analysis method used. Additionally, no significant differences were found between the normalized E* ratio calculated by the Oliver-Pharr Method vs. the Hertzian Method, the latter of which utilizes a modification that allows for E* to be calculated without a known contact depth or area. Therefore, overall, this points to an alternative and/or additional mechanism that is driving the stiffening response. This finding is also in agreement with our previous study, where the same stiffening response was assessed in surface-intact vs. surface-removed explants [12]. In both experimental groups, post-loading, the samples exhibited similar increases in load during the hold phase. Interestingly, however, surface-removed explants exhibited no increases in stiffness after articular loading, despite this same observed increase in force. While the mechanisms driving stiffening are currently unknown, in future work, it is necessary to

uncover these mechanisms to fully comprehend the observations of this study.

This study has other limitations that also need to be considered. Indents within each array were performed 100 μm apart, regardless of tip size. Therefore, for the larger tips, deformation caused by a previous consecutive indent could lead to potential error in the indentation measurement if the tissue does not relax in the time between indents. The idealized Hertzian contact radii (assuming a true sphere and an elastic half-space) for the 20, 100, and 793.75 μm tip sizes are 12.65, 28.28, 79.69 μm, respectively. Thus, especially in the case of the largest tip, the areas of contact of adjacent indents overlap. However, the data of this experiment showed that there was no difference in coefficient of variation between tip sizes when all individual indents were considered, hence indicating that this caveat is minor. Another limitation of this study was the material inconsistency between tip materials due to the availability of indenter tips in this study. The largest tip size was a custom spherical alumina tip that was borrowed from a different laboratory, whereas the other two smaller tip sizes were commercially obtained and made of diamond. Based on the results of this study, it is likely a fluid vacuum effect caused the adhesion-like responses. To further confirm that the adhesion-like response is not due to molecular adhesion, further investigation would be necessary using a large tip made of diamond.

Conclusions

In this study, two commonly used indentation analysis methods, the Oliver-Pharr Method and the Hertzian Method, were compared for cartilage microindentation at varying length-scales. It was shown that at the indentation depths and strains applied, geometric linearity was generally observed across the length-scale assessed for both cartilage stiffness and stiffening. Overall, the Hertzian Method used in this study resulted in more consistent E* calculations across the length-scale investigated than that of the Oliver-Pharr Method. Notably, the E* values obtained using the 20 μm tip size were similar between the Oliver-Pharr Method and the Hertzian Method. Regardless of indentation analysis method used, cartilage stiffness ratios, which were obtained by normalizing E* values after articular loading to baseline values, were similar across the range of the length-scale investigated. This indicates that the loading induced stiffening response of the superficial zone of cartilage is not length-scale dependent, fulfilling linearity assumptions necessary to use the elastic contact models assessed in this study.

Acknowledgements The authors would like to acknowledge Tim Ovaert (University of Notre Dame) for lending us the large alumina spherical tip, and Steven Mell and Michel Laurent for statistical input. This work was in part funded by the National Institutes of Health R01 AR066635 (PI S. Maher, site co-PI M.A.W.).

Funding The research leading to these results received funding from the National Institutes of Health under Grant Agreement R01 AR066635.

Declarations

Conflict of Interests The authors have no conflicts of interest to declare that are relevant to the content of this article.

References

1. Kempson GE, Freeman MAR, Swanson SAV (1971) The determination of a creep modulus for articular cartilage from indentation tests on the human femoral head. J Biomech 4:239–250. https://doi.org/10.1016/0021-9290(71)90030-3
2. Appleyard R, Ghosh P, Swain M (1999) Biomechanical, histological and immunohistological studies of patellar cartilage in an ovine model of osteoarthritis induced by lateral meniscectomy. In: Osteoarthritis and cartilage. https://pubmed.ncbi.nlm.nih.gov/10329303/. Accessed 16 Oct 2020
3. Ferguson VL, Bushby AJ, Boyde A (2003) Nanomechanical properties and mineral concentration in articular calcified cartilage and subchondral bone. J Anat 203:191–202. https://doi.org/10.1046/j.1469-7580.2003.00193.x
4. Hyttinen MM, Töyräs J, Lapveteläinen T et al (2001) Inactivation of one allele of the type II collagen gene alters the collagen network in murine articular cartilage and makes cartilage softer. Ann Rheum Dis 60:262–268. https://doi.org/10.1136/ard.60.3.262
5. Han L, Grodzinsky AJ, Ortiz C (2011) Nanomechanics of the Cartilage Extracellular Matrix. Annu Rev Mater Res 41:133–168. https://doi.org/10.1146/annurev-matsci-062910-100431
6. Han G, Hess C, Eriten M, Henak CR (2018) Uncoupled poroelastic and intrinsic viscoelastic dissipation in cartilage. J Mech Behav Biomed Mater 84:28–34. https://doi.org/10.1016/j.jmbbm.2018.04.024
7. Mattice JM, Lau AG, Oyen ML, Kent RW (2006) Spherical indentation load-relaxation of soft biological tissues. J Mater Res 21:2003–2010. https://doi.org/10.1557/jmr.2006.0243
8. M Oyen 2015 Nanoindentation of Hydrated Materials and Tissues. Curr Opin Solid State Mater Sci 19. https://doi.org/10.1016/j.cossms.2015.03.001
9. Wahlquist JA, DelRio FW, Randolph MA et al (2017) Indentation mapping revealed poroelastic, but not viscoelastic, properties spanning native zonal articular cartilage. Acta Biomater 64:41–49. https://doi.org/10.1016/j.actbio.2017.10.003
10. McGann ME, Bonitsky CM, Ovaert TC, Wagner DR (2014) The effect of collagen crosslinking on the biphasic poroviscoelastic cartilage properties determined from a semi-automated microindentation protocol for stress relaxation. J Mech Behav Biomed Mater 34:264–272. https://doi.org/10.1016/j.jmbbm.2014.02.013
11. Moshtagh PR, Korthagen NM, van Rijen MHP et al (2018) Effects of non-enzymatic glycation on the micro- and nano-mechanics of articular cartilage. J Mech Behav Biomed Mater 77:551–556. https://doi.org/10.1016/j.jmbbm.2017.09.035
12. Yuh C, Laurent MP, Espinosa-Marzal RM et al (2021) Transient stiffening of cartilage during joint articulation: A microindentation

study. J Mech Behav Biomed Mater 113:104113. https://doi.org/10.1016/j.jmbbm.2020.104113
13. Oliver WC, Pharr GM (1992) An improved technique for determining hardness and elastic modulus using load and displacement sensing indentation experiments. J Mater Res 7:1564–1583. https://doi.org/10.1557/JMR.1992.1564
14. Mow VC, Kuei SC, Lai WM, Armstrong CG (1980) Biphasic Creep and Stress Relaxation of Articular Cartilage in Compression: Theory and Experiments. J Biomech Eng 102:73–84. https://doi.org/10.1115/1.3138202
15. Garcia M, Schulze KD, O'Bryan CS et al (2017) Eliminating the surface location from soft matter contact mechanics measurements. Tribology - Materials, Surfaces & Interfaces 11:187–192. https://doi.org/10.1080/17515831.2017.1397908
16. Han G, Eriten M (2018) Effect of relaxation-dependent adhesion on pre-sliding response of cartilage. R Soc Open Sci 5:172051. https://doi.org/10.1098/rsos.172051
17. Kohn JC, Ebenstein DM (2013) Eliminating adhesion errors in nanoindentation of compliant polymers and hydrogels. J Mech Behav Biomed Mater 20:316–326. https://doi.org/10.1016/j.jmbbm.2013.02.002
18. Ciavarella M, Joe J, Papangelo A, Barber JR (2019) The role of adhesion in contact mechanics. J R Soc Interface 16. https://doi.org/10.1098/rsif.2018.0738
19. Budday S, Nay R, de Rooij R et al (2015) Mechanical properties of gray and white matter brain tissue by indentation. J Mech Behav Biomed Mater 46:318–330. https://doi.org/10.1016/j.jmbbm.2015.02.024
20. Andriacchi TP, Koo S, Scanlan SF (2009) Gait Mechanics Influence Healthy Cartilage Morphology and Osteoarthritis of the Knee. J Bone Joint Surg Am 91:95–101. https://doi.org/10.2106/JBJS.H.01408
21. Guilak F (2011) Biomechanical factors in osteoarthritis. Best Pract Res Clin Rheumatol 25:815–823. https://doi.org/10.1016/j.berh.2011.11.013
22. Ateshian GA (2009) The Role of Interstitial Fluid Pressurization in Articular Cartilage Lubrication. J Biomech 42:1163–1176. https://doi.org/10.1016/j.jbiomech.2009.04.040
23. Moore AC, Burris DL (2017) Tribological rehydration of cartilage and its potential role in preserving joint health. Osteoarthr Cartil 25:99–107. https://doi.org/10.1016/j.joca.2016.09.018
24. Wimmer MA, Grad S, Kaup T et al (2004) Tribology Approach to the Engineering and Study of Articular Cartilage. Tissue Eng 10:1436–1445. https://doi.org/10.1089/ten.2004.10.1436
25. Hertz H (1882) Ueber die Berührung fester elastischer Körper. Journal für die reine und angewandte Mathematik 1882:156–171. https://doi.org/10.1515/crll.1882.92.156
26. Johnson KL (1985) Contact Mechanics. In: Cambridge Core. /core/books/contact-mechanics/E3707F77C2EBCE727C3911AFBD2E4AC2. Accessed 16 Apr 2020
27. Tabor D (1951) The Hardness of Metals. Clarendon Press, Oxford
28. Sneddon IN (1965) The relation between load and penetration in the axisymmetric boussinesq problem for a punch of arbitrary profile. Int J Eng Sci 3:47–57. https://doi.org/10.1016/0020-7225(65)90019-4
29. Oyen ML (2013) Nanoindentation of Biological and Biomimetic Materials. Exp Tech 37:73–87. https://doi.org/10.1111/j.1747-1567.2011.00716.x
30. Grad S, Gogolewski S, Alini M, Wimmer MA (2006) Effects of simple and complex motion patterns on gene expression of chondrocytes seeded in 3D scaffolds. Tissue Eng 12:3171–3179. https://doi.org/10.1089/ten.2006.12.3171
31. Chen T, Wang H, Warren R, Maher S (2017) Loss of ACL function leads to alterations in tibial plateau common dynamic contact stress profiles. J Biomech 61:275–279. https://doi.org/10.1016/j.jbiomech.2017.07.024
32. Armstrong CG, Mow VC (1982) Variations in the intrinsic mechanical properties of human articular cartilage with age, degeneration, and water content. J Bone Joint Surg Am 64:88–94
33. Mow VC, Gibbs MC, Lai WM et al (1989) Biphasic indentation of articular cartilage—II. A numerical algorithm and an experimental study. J Biomech 22:853–861. https://doi.org/10.1016/0021-9290(89)90069-9
34. Schinagl RM, Gurskis D, Chen AC, Sah RL (1997) Depth-dependent confined compression modulus of full-thickness bovine articular cartilage. J Orthop Res 15:499–506. https://doi.org/10.1002/jor.1100150404
35. Waldstein W, Perino G, Gilbert SL et al (2016) OARSI osteoarthritis cartilage histopathology assessment system: A biomechanical evaluation in the human knee. J Orthop Res 34:135–140. https://doi.org/10.1002/jor.23010
36. Basalo IM, Mauck RL, Kelly T-AN et al (2004) Cartilage interstitial fluid load support in unconfined compression following enzymatic digestion. J Biomech Eng 126:779–786. https://doi.org/10.1115/1.1824123
37. Hosseini SM, Veldink MB, Ito K, van Donkelaar CC (2013) Is collagen fiber damage the cause of early softening in articular cartilage? Osteoarthr Cartil 21:136–143. https://doi.org/10.1016/j.joca.2012.09.002
38. Khoshgoftar M, Torzilli PA, Maher SA (2018) Influence of the Pericellular and Extracellular Matrix Structural Properties on Chondrocyte Mechanics. J Orthop Res 36:721–729. https://doi.org/10.1002/jor.23774
39. Nia HT, Han L, Li Y et al (2011) Poroelasticity of Cartilage at the Nanoscale. Biophys J 101:2304–2313. https://doi.org/10.1016/j.bpj.2011.09.011
40. Bolshakov A, Pharr GM (1998) Influences of pileup on the measurement of mechanical properties by load and depth sensing indentation techniques. J Mater Res 13:1049–1058. https://doi.org/10.1557/JMR.1998.0146